

Study on the poisoning tolerance and stability of perovskite catalysts for catalytic combustion of volatile organic compounds

Haifeng Huang · Zhong Sun · Hanfeng Lu ·
Liuqian Shen · Yinfei Chen

Received: 5 May 2010 / Accepted: 15 August 2010 / Published online: 9 September 2010
© Akadémiai Kiadó, Budapest, Hungary 2010

Abstract $\text{La}_{0.8}\text{Cu}_{0.2}\text{MnO}_3$ and $\text{La}_{0.8}\text{Sr}_{0.2}\text{MnO}_3$ perovskite catalysts were prepared by the co-precipitation method. The resistance of these catalysts to sulfur poisoning was tested via catalytic combustion of toluene. The results show that the perovskite catalysts were poisoned in the presence of SO_2 . In the presence of dodecyl mercaptan ($\text{C}_{12}\text{H}_{25}\text{SH}$), $\text{La}_{0.8}\text{Sr}_{0.2}\text{MnO}_3$ exhibits better resistance to sulfur poisoning than $\text{La}_{0.8}\text{Cu}_{0.2}\text{MnO}_3$. It was determined that the SO_2 deactivation is due to the formation of CuSO_4 on the catalyst surface.

Keywords VOCs · Catalytic combustion · Perovskite · Tolerance to poisoning · Stability

Introduction

Volatile organic compounds (VOCs) are considered to be significant environmental pollutants. Catalytic combustion is one of the most effective approaches to convert the diluted VOCs into harmless products such as CO_2 and H_2O [1]. Several catalyst systems have been used for VOC catalytic combustion, such as those incorporating noble metals and oxides of the transition metals [1, 2]. However, the VOCs from petrochemical, pesticide and foodstuff industries always contain some heteroatoms such as nitrogen, sulfur and chlorine [3, 4]. One problem concerning the normal noble metal catalysts is their sensitivity to poisoning due to the presence of sulfur

H. Huang · Z. Sun · L. Shen
College of Biological and Environmental Engineering, Zhejiang University of Technology,
Hangzhou 310032, People's Republic of China

H. Lu · Y. Chen (✉)
College of Chemical Engineering and Materials Science, Zhejiang University of Technology,
Hangzhou 310032, People's Republic of China
e-mail: yfchen@zjut.edu.cn

compounds and chlorine compounds in industrial organic exhaust gas [5–7]. The perovskite structure is characterized by a large capacity to stabilize unusual valence states of different metal ions and can also accommodate variable amounts of different lattice defects. Perovskite-type catalysts for VOC catalytic combustion are widely studied [8]. Several lanthanum transition metal based perovskites show very good oxidation performance in VOC combustion and they can be further enhanced by substitution of lanthanum by strontium or copper [9–12]. However, most of the oxide catalysts, including perovskites, are expected to be sensitive to sulfur and chlorine poisoning [13–15]. Lanthanum oxide, due to its basicity, has a tendency to form sulfate, sulfite and chloride. These unstable surface species, which probably lead to deactivation, have already been investigated [16–20].

It is thus significant to clarify the poisoning mechanism and the internal factors of catalyst deactivation in order to propose the practical composition of perovskite-based catalysts with better resistance to sulfur and chlorine poisoning. A primary sulfur poisoning mechanism was proposed in early publications, which displayed two distinct stages depending on poisoning time [21, 22]. At the first stage, a reversible minor deactivation was observed and chemisorptions of sulfur containing species at anion vacancies of perovskite surface interact with the accessible perovskite surface, which led to the formation of minor amounts of sulfate and sulfite over the perovskite surface. At the second stage, there is a deeper irreversible deactivation while large amounts of sulfate and sulfite formed and a linear diminution of conversion with time occurs and the perovskite structure was destroyed. Previous studies showed that Sr-doping increases the mobility of lattice oxygen of the perovskites [23–25]. Otherwise, the acid character of a metal ion increases with its oxidation state, the bonding of sulfur with the perovskite surface might be weakened [20, 26].

Based on the above summarized topics, $\text{La}_{0.8}\text{Cu}_{0.2}\text{MnO}_3$ and $\text{La}_{0.8}\text{Sr}_{0.2}\text{MnO}_3$ perovskite catalysts were prepared by the co-precipitation method in the present study. Resistance to sulfur poisoning of these catalysts was tested via VOC catalytic combustion. The mechanism of deactivation caused by sulfur poisoning was studied by X-ray diffraction (XRD) and X-ray photoelectron spectroscopic (XPS) techniques.

Experimental

Catalysts preparation

$\text{La}_{0.8}\text{Cu}_{0.2}\text{MnO}_3$ and $\text{La}_{0.8}\text{Sr}_{0.2}\text{MnO}_3$ were prepared via the co-precipitation method [8]. In a typical process, stoichiometric amounts of $\text{La}(\text{NO}_3)_3 \cdot 6\text{H}_2\text{O}$, $\text{Mn}(\text{NO}_3)_3 \cdot 4\text{H}_2\text{O}$, and $\text{Cu}(\text{NO}_3)_2$ or $\text{Sr}(\text{NO}_3)_2$ were dissolved in deionized water. The solution was stirred at 313 K in a water bath. A 25% ammonia solution was introduced as the precipitator. The pH value of the solution was adjusted to 11. The solution was then allowed to stand at room temperature for 24 h, the solid was washed by deionized water, and dried at 353 K for 24 h. The resulting powder was calcined at 973 K for 6 h. After grinding and sieving, $\text{La}_{0.8}\text{Cu}_{0.2}\text{MnO}_3$ and $\text{La}_{0.8}\text{Sr}_{0.2}\text{MnO}_3$ were obtained in their final form [8].

Catalytic performance test

The catalyst resistance to poisoning was tested in a fixed-bed continuous-flow micro-reactor at atmospheric pressure. The catalyst (154.2 mg, 500–750 μm particle size fraction) was diluted with quartz at a 1:10 quality ratio. The catalytic performance tests were carried out in the electric-heated reactor. The reaction temperature inside the catalytic bed was measured with a K-type thermocouple. The feed gas was composed of VOCs (toluene) and diluent gas (air). The gas flow space velocity (GHSV) was 5000 h^{-1} for all tests, and the reactor operated at a constant combustion temperature of 573 K for the sulfur poisoning. The products were analyzed by on-line GLC analysis with a HP6890 (FID) equipped with an AT.SE-30 capillary column (30 m \times 0.25 mm) [27].

The catalyst stability was tested in a fixed-bed continuous-flow micro-reactor at atmospheric pressure. The reactor was operated at a constant combustion temperature of 573 K, with the inlet concentration of toluene at 6000 ppmV, and the gas flow space velocity (GHSV) at 5000 h^{-1} . Reactants and products were analyzed by an on-line gas chromatograph (HP6890) [27].

Characterization of catalysts

Powder X-ray diffraction (XRD) patterns of the catalysts were recorded on a SCINTAG X'TRA X-ray powder diffractometer using Cu K_{α} radiation. Diffraction patterns were recorded over a 2θ range of 20–80°. The scan speed was 4° min^{-1} at 40 kV and 30 mA.

The specific surface area was measured by the BET method using N_2 on all fresh $\text{La}_{0.8}\text{Cu}_{0.2}\text{MnO}_3$ and $\text{La}_{0.8}\text{Sr}_{0.2}\text{MnO}_3$ catalysts (Micromeritics ASAP 2010 M apparatus). $\text{La}_{0.8}\text{Cu}_{0.2}\text{MnO}_3$ catalysts have a specific surface area of 21 $\text{m}^2 \text{g}^{-1}$, and $\text{La}_{0.8}\text{Sr}_{0.2}\text{MnO}_3$ catalysts have a specific surface area of 23 $\text{m}^2 \text{g}^{-1}$.

X-ray photoelectron spectroscopic (XPS) analysis was conducted using a PHI5300 analyzer (PHI, USA) employing Mg K_{α} radiation. All spectra were calibrated using the binding energy of C 1s (284.6 eV) as a reference.

Results and discussion

Catalyst tests on resistance to sulfur poisoning

The catalytic conversion of toluene containing SO_2 was tested to find the catalyst resistance to inorganic sulfur poisoning. The feed gas was composed of toluene (6000 ppmV) and varying concentrations of SO_2 . The GHSV was 5000 h^{-1} and the reaction temperature was maintained at 573 K.

Figs. 1 and 2 show that the conversion of toluene is greater than 80% in the presence of low concentrations (≤ 10 ppmV) of SO_2 . However, as the SO_2 concentration increased, the conversion rate of toluene decreased to some degree for both catalysts. Moreover, greater SO_2 concentrations resulted in markedly larger

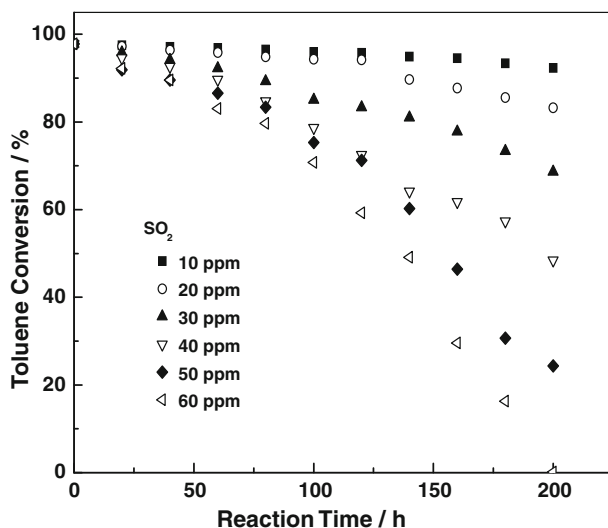


Fig. 1 Resistance to SO_2 of the $\text{La}_{0.8}\text{Cu}_{0.2}\text{MnO}_3$ catalyst ([toluene] = 6000 ppmV, GHSV = 5000 h^{-1} , $T = 573$ K, $[\text{SO}_2] = 10\text{--}60$ ppmV)

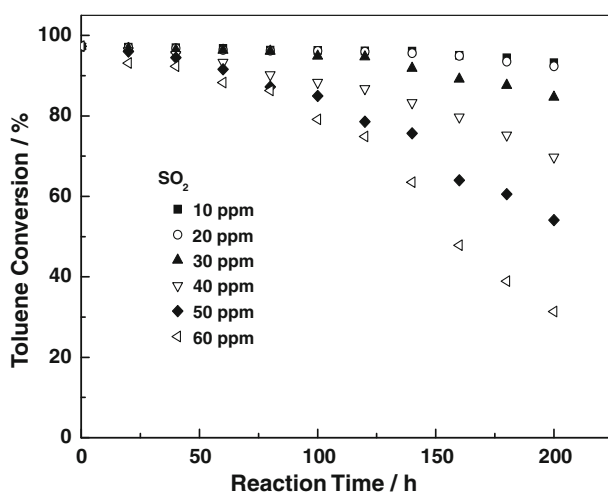


Fig. 2 Resistance to SO_2 of the $\text{La}_{0.8}\text{Sr}_{0.2}\text{MnO}_3$ catalyst ([toluene] = 6000 ppmV, GHSV = 5000 h^{-1} , $T = 573$ K, $[\text{SO}_2] = 10\text{--}60$ ppmV)

decreases in toluene conversion. When the SO_2 concentration was 60 ppmV, the $\text{La}_{0.8}\text{Cu}_{0.2}\text{MnO}_3$ catalyst was nearly completely deactivated after 200 h.

There are few reports on the recovery of catalysts after sulfur poisoning. In this study, the catalysts were reset into the reactor after being poisoned by SO_2 of 60 ppmV to investigate the regeneration ability of these catalysts. Tests were performed under the same reaction conditions of toluene catalytic combustion with SO_2 concentration ranging from 50 to 10 ppmV. The results are shown in Figs. 3

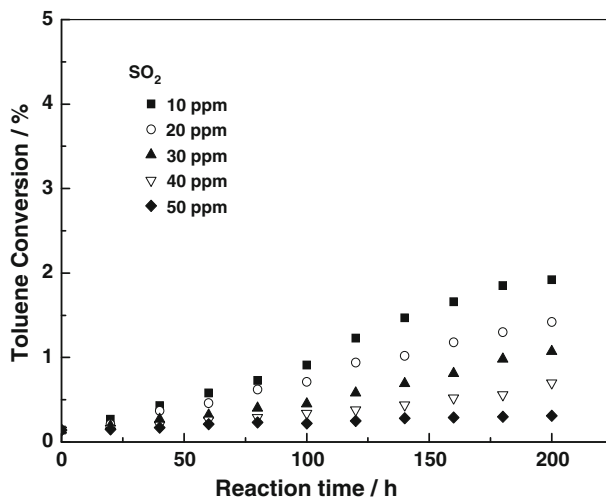


Fig. 3 Recovery of the poisoned $\text{La}_{0.8}\text{Cu}_{0.2}\text{MnO}_3$ catalyst ([toluene] = 6000 ppmV, GHSV = 5000 h^{-1} , $T = 573$ K, $[\text{SO}_2] = 50\text{--}10$ ppmV)

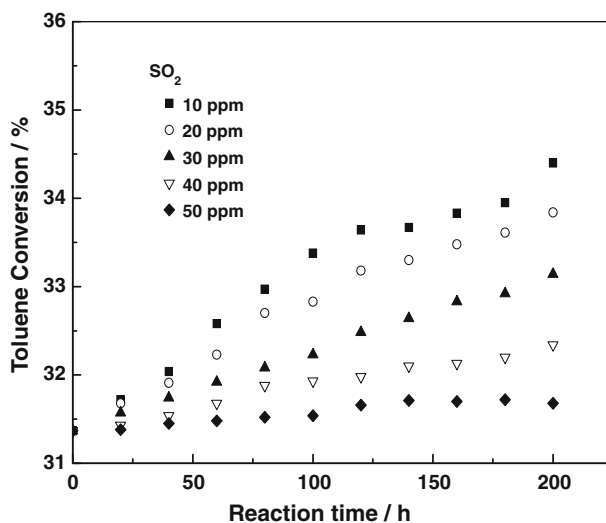


Fig. 4 Recovery of the poisoned $\text{La}_{0.8}\text{Sr}_{0.2}\text{MnO}_3$ catalyst ([toluene] = 6000 ppmV, GHSV = 5000 h^{-1} , $T = 573$ K, $[\text{SO}_2] = 50\text{--}10$ ppmV)

and 4. The toluene conversion of the deactivated catalysts cannot be recovered over 200 h with 10–50 ppmV SO_2 in the feed gas. At 10 ppmV SO_2 , toluene conversion on poisoned $\text{La}_{0.8}\text{Cu}_{0.2}\text{MnO}_3$ increased from 0 to 1.8% and from 31.5 to 34.5% for $\text{La}_{0.8}\text{Sr}_{0.2}\text{MnO}_3$. It is indicated that the recovery of poisoned catalysts is easier when the SO_2 concentration is lower.

We also investigated the catalyst resistance to organic sulfur poisoning by testing the catalytic toluene conversion of containing $\text{C}_{12}\text{H}_{25}\text{SH}$. The feed gas was composed

of toluene (6000 ppmV) and different concentrations of $C_{12}H_{25}SH$, and the reaction conditions were identical to those of the SO_2 test. The conversion rates of toluene with the two catalysts in the presence of $C_{12}H_{25}SH$ are shown in Figs. 5 and 6. The conversion rate of toluene with $La_{0.8}Cu_{0.2}MnO_3$ decreased as the concentration of $C_{12}H_{25}SH$ increased. Higher $C_{12}H_{25}SH$ concentrations caused faster decreases to the conversion rate. The conversion rate of toluene with $La_{0.8}Sr_{0.2}MnO_3$ was steady above 95%, even though the $C_{12}H_{25}SH$ concentration was varied. The $La_{0.8}Sr_{0.2}MnO_3$ had better $C_{12}H_{25}SH$ resistance than $La_{0.8}Cu_{0.2}MnO_3$.

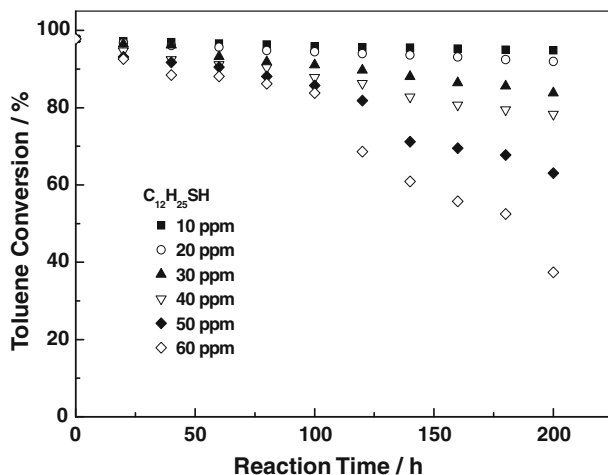


Fig. 5 Resistance to $C_{12}H_{25}SH$ of the $La_{0.8}Cu_{0.2}MnO_3$ catalyst ([toluene] = 6000 ppmV, GHSV = 5000 h^{-1} , $T = 573$ K, $[C_{12}H_{25}SH] = 10\text{--}60$ ppmV)

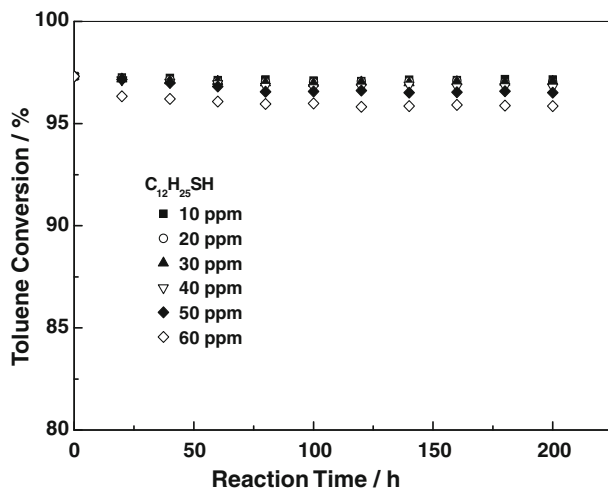


Fig. 6 Resistance to $C_{12}H_{25}SH$ of the $LaSr_{0.2}Mn_{0.8}O_3$ catalyst ([toluene] = 6000 ppmV, GHSV = 5000 h^{-1} , $T = 573$ K, $[C_{12}H_{25}SH] = 10\text{--}60$ ppmV)

Catalyst tests on resistance to chlorine poisoning

Tests of catalytic performance over dichloromethane were conducted to find the catalyst resistance to chlorine poisoning. The inlet concentration of dichloromethane was 3000 ppmV. The reaction was carried out at the GHSV of 5000 h^{-1} at 693 K. As shown in Fig. 7, the conversions of dichloromethane during 200 h reaction were maintained above 96%. This indicates that the catalysts have good tolerance to chlorine poisoning.

Catalytic stability test

The catalytic stability of the $\text{La}_{0.8}\text{Cu}_{0.2}\text{MnO}_3$ and $\text{La}_{0.8}\text{Sr}_{0.2}\text{MnO}_3$ was tested under the following conditions: The concentration of toluene as feed gas is 2400 ppmV with GHSV 5000 h^{-1} and reaction temperature 573 K.

The results plotted in Fig. 8 suggest that the conversion of toluene gradually decreases on the Cu-catalyst during 200 h of testing, but is still maintained above 95%. Comparatively, the performance of Sr-catalyst exhibits better catalytic stability during a 200-h test.

Deactivation mechanism

XRD characterization

The XRD patterns of catalysts samples are shown in Figs. 9 and 10. As can be seen in the XRD patterns of fresh Cu-catalyst and Sr-catalyst, regular diffraction peaks at $2\theta = 23.0^\circ, 32.7^\circ, 47.0^\circ, 58.0^\circ$ are observed. These peaks correspond to the standard patterns of perovskite phase [8]. The XRD patterns of poisoned Cu-catalyst

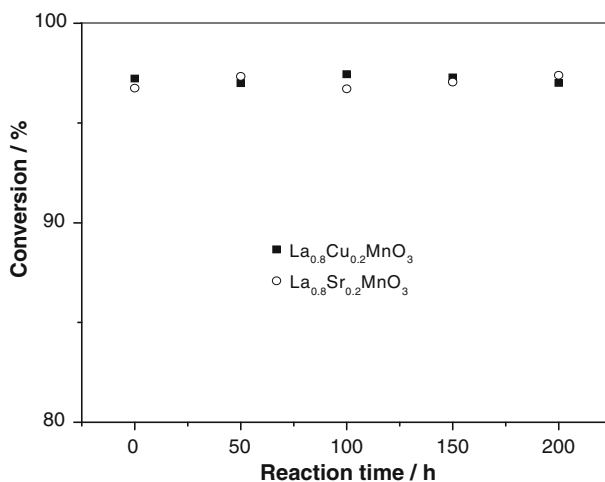


Fig. 7 Resistance to chlorine of the $\text{La}_{0.8}\text{Sr}_{0.2}\text{MnO}_3$ and $\text{La}_{0.8}\text{Cu}_{0.2}\text{MnO}_3$ catalysts ([dichloromethane] = 3000 ppmV, GHSV = 5000 h^{-1} , $T = 693 \text{ K}$)

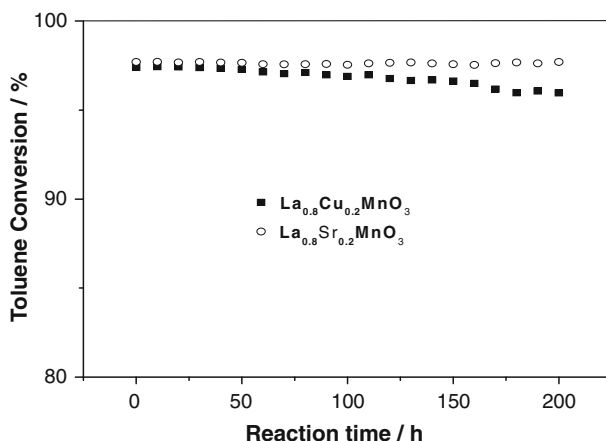


Fig. 8 Stability of the La_{0.8}Sr_{0.2}MnO₃ and La_{0.8}Cu_{0.2}MnO₃ catalysts ([toluene] = 6000 ppmV, GHSV = 2000 h⁻¹, *T* = 573 K)

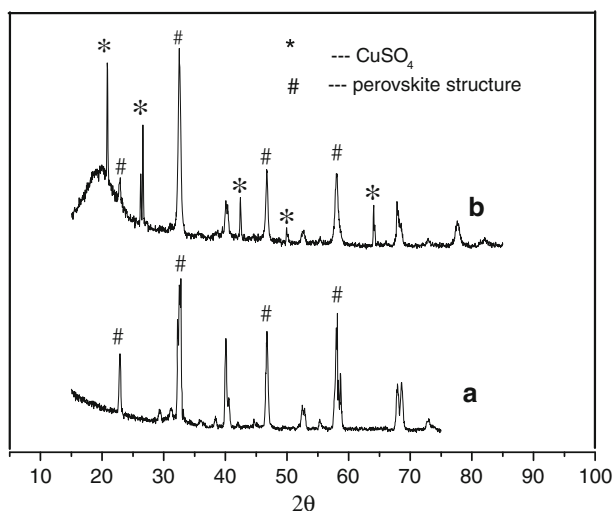


Fig. 9 XRD patterns of La_{0.8}Cu_{0.2}MnO₃ samples. (a) The sample before reaction. (b) The sample after reacting with SO₂

are shown in Fig. 9. The dispersion of peaks at 2θ of 15–25° suggests that the perovskite crystal structure has been destroyed and amorphous phase forms partially. According to the JCPDS card, the diffraction peaks at $2\theta = 21^\circ, 42^\circ, 50^\circ, 64^\circ$ correspond to the CuSO₄ crystal phase. Similarly, the XRD patterns of poisoned Sr-catalyst plotted in Fig. 10 show dispersion of peaks at $2\theta = 15\text{--}25^\circ$, suggesting that there is an amorphous phase existed. The perovskite crystal structure has been destroyed slightly as well. Comparatively, there are no crystal diffraction peaks of SrSO₄ or other compounds.

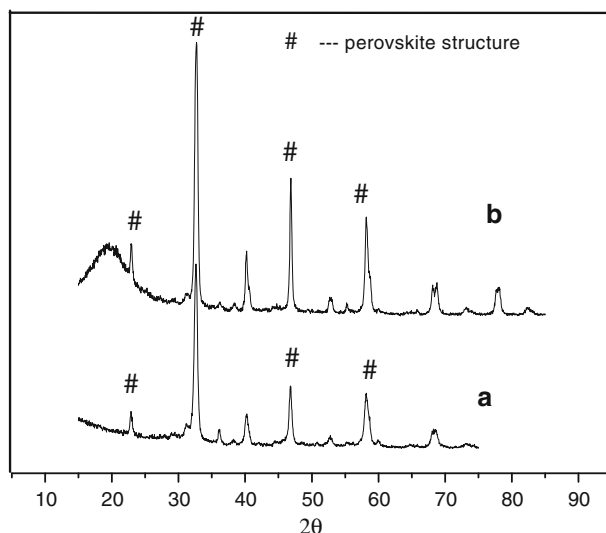


Fig. 10 XRD patterns of $\text{La}_{0.8}\text{Sr}_{0.2}\text{MnO}_3$ samples. (a) The sample before reaction. (b) The sample after reacting with SO_2

With reference to Figs. 1 and 2, the catalytic performance of Sr-catalyst decreased in the presence of SO_2 , but less significantly than that of Cu-catalyst. This suggests that Sr-catalyst has better structure stability than Cu-catalyst.

XPS characterization

XPS characterization analysis of the poisoned catalysts was applied to investigate the SO_2 poisoning mechanism. The XPS signal of S and the binding energy shift of each element on the poisoned catalyst surface are shown in Tables 1 and 2. It can be seen in the S 2p high resolution XPS spectra of the Cu-catalyst that there is a peak S2 at a binding energy of 169.7 eV. Its position (169.5 eV for S of CuSO_4 in the standard spectra) corresponds to the XPS signal for the S of CuSO_4 [28]. Comparatively, there is a peak S1 at a binding energy of 166.7 eV (168.4 eV for S of SrSO_4 in the standard spectra) in the S 2p high-resolution XPS spectra of the Sr-catalyst show that SrSO_4 is quite not detectable on the Sr-perovskite.

Table 1 Binding energies of catalysts before and after poisoning (eV)

	C (1s)	La (3d)	Mn (2p)	S (2p)	Cu (2p)	Sr (3d)	O (1s)
$\text{La}_{0.8}\text{Cu}_{0.2}\text{MnO}_3$							
Fresh	287.5	834.5	642.5	–	942.0	–	529.1
Poisoned	287.8	834.9	642.1	169.7	935.7	–	533.0
$\text{La}_{0.8}\text{Sr}_{0.2}\text{MnO}_3$							
Fresh	284.4	835.1	642.3	–	–	132.9	529.5
Poisoned	285.7	835.9	642.2	166.7	–	133.2	531.1

Table 2 Atomic concentrations on the catalyst surface (%)

	La (1s)	Mn (2p)	S (2p)	Cu (2p)	Sr (3d)	O (1s)	C (1s)
La_{0.8}Cu_{0.2}MnO₃							
Fresh	4.0	3.7	0	1.6	–	35.7	56.0
Poisoned	3.5	6.6	0.7	0.7	–	45.8	42.6
La_{0.8}Sr_{0.2}MnO₃							
Fresh	6.7	14.3	0	–	1.44	46.0	31.0
Poisoned	4.5	10.1	2.4	–	2.14	49.0	32.6

The obvious binding energy shift between Cu and O in the fresh and poisoned Cu-catalysts is due to the formation of CuSO₄ crystals at the surface of the Cu-catalyst. Comparatively, the binding energy shift between Sr and O is smaller than that of the Cu-catalyst, which indicates that less SrSO₄ forms on the catalyst surface, and that the Sr-catalyst exhibits good stability. The Sr-catalyst exhibits better resistance to sulfur poisoning than the Cu-catalyst.

Conclusion

La_{0.8}Cu_{0.2}MnO₃ and La_{0.8}Sr_{0.2}MnO₃ perovskite catalysts were prepared by the co-precipitation method. Testing for resistance to sulfur poisoning indicated that La_{0.8}Sr_{0.2}MnO₃ exhibited better resistance to sulfur poisoning than La_{0.8}Cu_{0.2}MnO₃ in the presence of dodecyl mercaptan (C₁₂H₂₅SH). The toluene conversions decreased to some degree for both catalysts as the SO₂ concentration in the mixture increased. It can be concluded that the catalyst poisoning in the presence of SO₂ is due to the formation of CuSO₄ and SrSO₄, which are generated by combining SO₂ and the metal ion in the two catalysts. The screening effect of CuSO₄ on the catalyst surface leads directly to the deactivation.

Tests of catalytic performance over dichloromethane were conducted to find the tolerance of catalysts to chlorine poisoning. This indicated that the two catalysts showed good tolerance to chlorine poisoning. The 200-h catalytic stability tests demonstrated that the two catalysts exhibited good stability and the Sr-catalyst performed better than the Cu-catalyst. The conversions of toluene were maintained above 95%.

Acknowledgment The authors thank the Zhejiang Provincial Science and Technology Office (2007C13042) in China for their financial support.

References

1. Domeno C, Rodrtguez A, Martos JM, Bilbao R, Nerin C (2010) *Environ Sci Technol* 44:2585–2591
2. Konig G, Brunda M, Puxbaum H, Hewitt CN, Duckham SC, Rudolph J (1995) *Atmos Environ* 29(8):861–874
3. Jindal K, Bhattacharyab D, Francisa LF, McCormick AV, Germinario LT, Williams C (2010) *Prog Org Coat* 67:296–301

4. Musialik-Piotrowska A (2007) *Catal Today* [J] 119:301–304
5. Lewisa CW, Zweidinger RB (1992) *Atmos Environ Part A Gen Top* 26(12):2179–2184
6. Yu T, Shaw H (1998) *Appl Catal B: Environ* [J] 18:105–114
7. Wakita H, Kani Y, Ukai K (2005) *Appl Catal A: Gen* [J] 283:53–61
8. Yang X, Luo L, Zhong H (2004) *Appl Catal A: Gen* 272:299–303
9. Ciambelli P, Cimino S, De Rossi S, Lisi L, Minelli G, Porta P, Russo G (2000) *Appl Catal B: Environ* [J] 1:757
10. Ciambelli P, Cimino S, De Rossi S, Faticanti M, Lisi L, Minelli G, Pettiti I, Porta P, Russo G, Turco M (2000) *Appl Catal B: Environ* [J] 24:243
11. Saracco G, Geobaldo F, Baldi G (1999) *Appl Catal B: Environ* [J] 20:277
12. Arai H, Yamada T, Eguchi K, Seiyama T (1986) *Appl Catal* [J] 26:265
13. Zhua Y, Tan R, Feng J, Ji S, Cao L (2001) *Appl Catal A: Gen* [J] 209:71–77
14. Musialik-Piotrowska A, Syczewska K (2002) *Catal Today* [J] 73:333–342
15. Tejuca LJ, Fierro JLG, Tascon JMD (1989) In: Eley DD, Pines H, Weisz PB (eds) *Advances in catalysis*, vol 36, p 237
16. Alifanti M, Auer R, Kirchnerova J, Thyron F, Grange P, Delmona B (2003) *Appl Catal B: Environ* [J] 41:71–81
17. Koponen MJ, Venalainen T, Suvanto M, Kallinen K, Kinnunen T, Harkonen M, Pakkanen TA (2006) *J Mol Catal A: Chem* [J] 258:246–250
18. Rosso I, Garrone E, Geobaldo F (2001) *Appl Catal B: Environ* [J] 30:61–73
19. Rosso I, Garrone E, Geobaldo F (2001) *Appl Catal B: Environ* [J] 34:29–41
20. Rossetti I, Buchneva O, Biffi C, Rizza R (2009) *Appl Catal B: Environ* [J] 89:383–390
21. Zhang R, Alamdari H, Kaliaguine S (2008) *Appl Catal A: Gen* [J] 340:140–151
22. Royer S, Neste AV, Davidson R, McIntyre S, Kaliaguine S (2004) *Ind Eng Chem Res* [J] 43:5670
23. Gaillard F, Joly JP, Li N, Boreave A, Deloume JP (2008) *Solid State Ionics* [J] 179:941–945
24. Mai A, Tietz F, Ster D (2004) *Solid State Ionics* [J] 173:35–40
25. Alifanti M, Kirchnerova J, Delmon B, Klvana D (2004) *Appl Catal A: Gen* [J] 262:167–176
26. Nakamura T, Misono M, Yoneda Y (1983) *J Catal* 83:151
27. Zhang S (2000) *Admin Tech Environ Monit (China)* [J] 3(12):33–34
28. NIST X-ray Photoelectron Spectroscopy Database [S]. <http://srdata.nist.gov/xps/XPSDetailPage.aspx?AllDataNo=44610>